THE JOURNAL OF BIOLOGICAL CHEMISTRY VOL. 284, NO. 21, pp. 14189–14202, May 22, 2009

Structure of a Viral Cap-independent Translation Element That Functions via High Affinity Binding to the eIF4E Subunit of eIF4F*[S]

Received for publication, November 21, 2008, and in revised form, March 9, 2009 Published, JBC Papers in Press, March 10, 2009, DOI 10.1074/jbc.M808841200

Zhaohui Wang[‡], Krzysztof Treder[‡1], and W. Allen Miller[‡§2]

From the Departments of [‡]Plant Pathology and [§]Biochemistry, Biophysics, and Molecular Biology, Iowa State University, Ames, Iowa 50011

RNAs of many positive strand RNA viruses lack a 5′ cap structure and instead rely on cap-independent translation elements (CITEs) to facilitate efficient translation initiation. The mechanisms by which these RNAs recruit ribosomes are poorly understood, and for many viruses the CITE is unknown. Here we identify the first CITE of an umbravirus in the 3′-untranslated region of pea enation mosaic virus RNA 2. Chemical and enzymatic probing of the ~100-nucleotide PEMV RNA 2 CITE (PTE), and mutagenesis revealed that it forms a long, bulged helix that branches into two short stem-loops, with a possible pseudoknot interaction between a C-rich bulge at the branch point and a G-rich bulge in the main helix. The PTE inhibited translation in *trans*, and addition of eIF4F, but not eIFiso4F, restored translation. Filter binding assays revealed that the PTE binds eIF4F and its eIF4E subunit with high affinity. Tight binding required an intact cap-binding pocket in eIF4E. Among many PTE mutants, there was a strong correlation between PTE-eIF4E binding affinity and ability to stimulate cap-independent translation. We conclude that the PTE recruits eIF4F by binding eIF4E. The PTE represents a different class of translation enhancer element, as defined by its structure and ability to bind eIF4E in the absence of an m^{7}G cap.

Regulation of translation occurs primarily at the initiation step. This involves recognition of the 5′ m^{7}G(5′)ppp(5′)N cap structure on the mRNA by initiation factors, which recruit the ribosome to the 5′-end of the mRNA (1–5). The 5′ cap structure and the poly(A) tail are necessary for efficient recruitment of initiation factors on eukaryotic mRNAs (3, 6–8). The cap is recognized by the eIF4E subunit of eukaryotic translation initiation factor complex eIF4F (or the eIFiso4E subunit of eIFiso4F in higher plants). The poly(A) tail is recognized by poly(A)-binding protein. In plants, eIF4F is a heterodimer consisting of eIF4E and eIF4G, the core scaffolding protein to which the other factors bind. eIF4A, an ATPase/RNA helicase, interacts with eIF4F but is not part of the eIF4F heterodimer (9, 10). For translation initiation, the purpose of eIF4E is to bring eIF4G to the capped mRNA. eIF4G then recruits the 43 S ternary ribosomal complex via interaction with eIF3.

The RNAs of many positive sense RNA viruses contain a cap-independent translation element (CITE)[3] that allows efficient translation in the absence of a 5′ cap structure (11–13). In animal viruses and some plant viruses, the CITE is an internal ribosome entry site (IRES) located upstream of the initiation codon. Most viral IRESes neither interact with nor require eIF4E, because they lack the m^{7}GpppN structure, which, until this report, was thought to be necessary for mRNA to bind eIF4E with high affinity (3, 14). Translation initiation efficiency of mRNA is also influenced by the length of, and the degree of secondary structure in the 5′ leader (15–17).

Many uncapped plant viral RNAs harbor a CITE in the 3′-UTR that confers highly efficient translation initiation at the 5′-end of the mRNA (18–22). These 3′ CITEs facilitate ribosome entry and apparently conventional scanning at the 5′-end of the mRNA (17, 23, 24). A variety of unrelated structures has been found to function as 3′ CITEs, suggesting that they recruit the ribosome by different interactions with initiation factors (13).

The factors with which a plant CITE interacts to recruit the ribosome have been identified for only a potyvirus, a luteovirus, and a satellite RNA. The 143-nt 5′-UTR CITE of the potyvirus, tobacco etch virus is an IRES that functions by binding of its AU-rich pseudoknot structure with eIF4G (25). It binds eIF4G with up to 30-fold greater affinity than eIFiso4G and does not require eIF4E for IRES activity. In addition to RNA elements, the genome-linked viral protein (VPg) of potyviruses may participate in cap-independent translation initiation by interacting with the eIF4E and eIFiso4E subunits of eIF4F and eIFiso4F, respectively (26–31). In contrast, the 130-nt cap-independent

* This work was supported, in whole or in part, by National Institutes of Health Grant 2R01 GM067104. This is journal paper of the Iowa Agriculture and Home Economics Experiment Station, Ames, IA, Project No. 3608 was supported by Hatch Act and State of Iowa funds.

[S] The on-line version of this article (available at http://www.jbc.org) contains supplemental Figs. S1–S3.

[1] Current address: Laboratory of Molecular Diagnostic and Biochemistry, Dept. of Potato Protection and Seed Science, Plant Breeding and Acclimatization Institute, Bonin 3, 76-009 Bonin, Poland.

[2] To whom correspondence should be addressed: 351 Bessey Hall, Iowa State University, Ames, IA 50011. Tel.: 515-294-2436; Fax: 515-294-9420; E-mail: wamiller@iastate.edu.

[3] The abbreviations used are: CITE, cap-independent translation element; PTE, PEMV RNA 2 cap-independent translation element; IRES, internal ribosome entry site; nt, nucleotide(s); UTR, untranslated region; TED, translation enhancer domain; STNV, satellite tobacco necrosis virus; BYDV, barley yellow dwarf luteovirus; BTE, BYDV-like CITE; ORF, open reading frame; PEMV-1,2, pea enation mosaic viruses 1 and 2; Bis-Tris, 2-[bis(2-hydroxyethyl)amino]-2-(hydroxymethyl)propane-1,3-diol; NMIA, *N*-methylisatoic anhydride; DTT, dithiothreitol; GST, glutathione *S*-transferase; PTE, PEMV RNA 2 CITE; SHAPE, selective 2′-hydroxyl acylation analyzed by primer extension; PMV, panicum mosaic virus; MNSV, melon necrotic spot virus; TBTV, tobacco bushy top virus.

translation enhancer domain (TED) in the 3′-UTR of satellite tobacco necrosis virus (STNV) RNA forms a long bulged stem-loop, which interacts strongly with both eIF4F and eIFiso4F and weakly with their eIF4E and eIFiso4E subunits (32), suggesting that the TED requires the full eIF4F or eIFiso4F for a biologically relevant interaction. Barley yellow dwarf luteovirus (BYDV) and several other viruses, have a different structure, called a BYDV-like CITE (BTE), in the 3′-UTR. The BTE is characterized by a 17-nt conserved sequence incorporated in a structure with a variable number of stem-loops radiating from a central junction (20, 33, 34). It requires and binds the eIF4G subunit of eIF4F and does not bind free eIF4E, eIFiso4E, or eIFiso4G, although eIF4E slightly enhances the BTE-eIF4G interaction (35). Other 3′ CITEs have been identified, but the host factors with which they interact are unknown.

Here we describe unprecedented factor interactions of a CITE found in an umbravirus and a panicovirus. Umbraviruses show strong similarity to the *Luteovirus* and *Dianthovirus* genera in (i) the sequence of the replication genes encoded by ORFs 1 and 2, (ii) the predicted structure of the frameshift signals required for translation of the RNA-dependent RNA polymerase from ORF 2 (36, 37), (iii) the absence of a poly(A) tail, and (iv) the lack of a 5′ cap structure (37, 38). Umbraviruses are unique in that they encode no coat protein. For the umbravirus pea enation mosaic virus 2 (PEMV-2), the coat protein is provided by PEMV-1, an enamovirus (39). Uncapped PEMV-2 RNA (PEMV RNA 2), transcribed *in vitro*, is infectious in pea (*Pisum sativa*),[4] indicating it must be translated cap-independently. The 3′-UTRs of some umbraviruses such as Tobacco bushy top virus and Groundnut rosette virus harbor sequences resembling BYDV-like CITEs (BTE).[5] However, no BTE is apparent in the 3′-UTR of PEMV RNA 2. In this report we identify a different class of CITE in the 705-nt long 3′-UTR of PEMV RNA 2, determine its secondary structure, which may include an unusual pseudoknot, and we show that, unlike any other natural uncapped RNA, it has a high affinity for eIF4E, which is necessary to facilitate cap-independent translation.

EXPERIMENTAL PROCEDURES

Plasmid Constructs and RNA Preparation by in Vitro Transcription—pPER2 is a plasmid containing PEMV RNA 2 cDNA (38). P2lucP2 is a reporter RNA transcribed from plasmid pP2lucP2 (Fig. 1*C*) consisting of the firefly luciferase gene (luc2, Promega) flanked by the 5′- and 3′-UTRs of PEMV RNA 2. The 20-nt 5′-UTR was fused directly between the T7 promoter and the luciferase start codon by PCR. The resulting construct has only viral 5′-UTR sequence upstream of the luciferase coding region. The 3′-UTR was inserted adjacent to the luciferase ORF stop codon with a unique XbaI restriction endonuclease site. Site-directed mutagenesis by overlap extension PCR was applied to generate mutant constructs: segments were amplified with mutations introduced into the primers sequences and placed back onto the 3′-UTR of the luciferase reporter construct to replace the wild-type sequence by using XbaI and SmaI, XbaI and SalI, or SalI and EagI sites (Fig. 1). Resulting constructs were verified by sequencing at the Iowa State University DNA Sequencing Facility.

All reporter constructs were linearized with SmaI, unless specified otherwise, as templates for RNA preparation. RNAs were transcribed *in vitro* with bacteriophage T7 or SP6 polymerase using a mMESSAGE mMACHINE™ kit for capped RNAs or MEGAscript™ for uncapped RNAs according to the manufacturer's instruction (Ambion). MEGAshortscript™ was used to transcribe the PTE element for structure probing, *trans*-inhibition, and filter binding assays. RNA integrity was verified by 0.8% agarose gel electrophoresis and then purified according to the manufacturer's instructions. RNA concentration was determined by spectrophotometry.

Translation in Vitro and in Protoplasts—In Vitro translation was set up in wheat germ extract with either [^{35}S]methionine (genomic RNAs and its truncations) or unlabeled amino acids mixture (luciferase reporter RNAs). 1.6 pmol of RNA transcript from pPER2 linearized with SmaI, SacII, or HpaI was translated in 50 μl of wheat germ extract (Promega, Madison, WI) essentially as described by the manufacturer, except no additional potassium acetate was added (for maximal expression). Products were separated on a NuPAGE® 4–12% Bis-Tris gel (Invitrogen), detected with a Pharos FX™ plus Molecular Imager and quantified by Quantity One one-dimensional analysis software (Bio-Rad). For translation of luciferase reporter RNA, 0.4 pmol of RNA was translated in wheat germ extract in a total volume of 50 μl with unlabeled amino acids mixture. In RNA competition experiments, the reporter RNA was mixed with the designated amount of competitor RNA prior to adding it to the translation reaction. After 1-h incubation at room temperature, the luciferase activity was measured using the luciferase assay reporter system (Promega) in a TD 20/20 luminometer (Turner Designs) or a GloMax™ 20/20 luminometer (Promega).

For translation *in vivo* (protoplasts) 2 pmol of uncapped RNA transcript from pP2lucP2 or its derived mutants was mixed with 0.2 pmol of capped and poly(A)$_{60}$-tailed *Renilla*-luciferase reporter mRNA (34) and electroporated into ~10^6 oat (*Avena sativa* cv. Stout) protoplasts, which were prepared basically as described (38, 40). After 4-h incubation at room temperature, protoplasts were harvested and lysed in Passive Lysis Buffer (Promega). Both *Renilla* and firefly luciferase activities were measured using Dual-Luciferase® reporter assay system (Promega). To minimize variations among electroporations, the firefly luciferase activities were normalized to the *Renilla* luciferase. The relative activity obtained from P2lucP2, after normalization, was defined as 100%.

RNA Structure Probing—An RNA segment comprising bases 3777–3982 (with extra GAA sequence at the 5′-end for optimal SP6 RNA polymerase activity, referred to as PTE$_{3777-3982}$ herein) was transcribed *in vitro* directly from a PCR product using a MEGAscript® SP6 kit, purified by phenol-chloroform extraction and ammonium acetate-ethanol precipitation according to the instructions in the kit. RNA (500 ng per reaction) was denatured at 94 °C for 1 min then chilled quickly on ice for 2 min. The RNA was renatured by incubation at room

[4] Z. Wang, unpublished observation.
[5] Z. Wang and W. A. Miller, unpublished observation.

temperature for 40 min in the buffer SHAPE (50 mM HEPES-KOH, pH 7.2, 100 mM KCl, 8 mM $MgCl_2$). *N*-Methylisatoic anhydride (NMIA) modification was performed essentially according to methods used previously (41, 42), except buffer SHAPE was applied to mimic the buffer used in translation and filter binding assays. RNase ONE (Promega) digestion (0.025–0.1 unit per reaction) was carried out at 20 °C for 15 min in the presence of yeast tRNA (2.0 μg per reaction) in buffer SHAPE. Primer (GATCTTTTTGGGCGAGACATC, complementary to nt 3830–3850 (Fig. 3*A*)) labeled at the 5′-end with γ-[^{32}P]ATP was used for the extension reaction as described in a previous study (42) except 20 units of Superscript™ II reverse transcriptase (Invitrogen) was used per reaction. After TBE urea 8% polyacrylamide gel electrophoresis and autoradiography, the nucleotide positions were identified by reference to the sequencing ladder from unmodified RNA by Sanger methods. RNA secondary structure was deduced from solution probing results and the best fitting Mfold prediction (43).

Recombinant Protein Expression and Purification—Recombinant wheat eIF4F and eIFiso4F were purified as described before (35, 44). For construction of the eIF4G expression vector, the coding sequence from the eIF4F expression vector (44) with extra sequence GAAAACCTGTATTTTCAGTCT (encoding tobacco etch virus proteinase reorganization peptide, ENLYFQS) upstream of start codon was amplified and introduced into the BamHI/XhoI sites of pET28a vector (Novagen). The construct was confirmed by DNA sequencing and designated as pETw4G. Protein expression was performed in *Escherichia coli* BL21(DE3) cells and induced with 1 mM isopropyl-β-D-thiogalactopyranoside at 30 °C for 4 h. Expressed eIF4G was first purified through a phosphocellulose column (44), followed by HisPur Cobalt Resin (Pierce) column purification, essentially as instructed by the manufacturer, except buffer N-300 (25 mM HEPES-KOH, pH 7.6, 300 mM KCl, 10% glycerol) plus 10 mM imidazole was used for equilibration and washing, and buffer N-300 plus 150 mM imidazole for elution. The eluted protein was concentrated and further purified by gel-filtration chromatography through Sephacryl™ S-200 (Amersham Biosciences). The desired portion was collected and dialyzed against N-100 (25 mM HEPES-KOH, pH 7.6, 100 mM KCl, 10% glycerol) plus 1 mM DTT. eIF4E was either purified through Illustra™ m^{7}GTP Sepharose (Amersham Biosciences) according to the procedure described before (44) or as a GST fusion. For expression and purification of eIF4E from the GST fusion, the coding region of wheat eIF4E with N-terminal modification, but maintaining the correct amino acid sequence (45), was amplified and cloned into the BamHI/EcoRI sites of pGEX2T (Amersham Biosciences). The construct was confirmed by DNA sequencing and designated as pETw4E. Site-directed mutagenesis by overlap extension PCR was applied to amplify two mutant versions of eIF4E (G323U and G185U/G323U), which altered one or both of the tryptophan residues in the cap-binding pocket to leucine (W108L and W62L/W108L). They were inserted back into the PGEXw4E vector to replace the wild-type eIF4E coding sequence. The resulting construct was confirmed by DNA sequencing and designated as PGEXw4E W108L and PGEXw4E W62L/W108L, respectively. *E. coli* BL21(DE3) was used to express GST-tagged eIF4E or the mutant following induction with 0.2 mM isopropyl-β-D-thiogalactopyranoside at 30 °C for 6 h. The cell pellet was sonicated in buffer N-100 plus 1 mM DTT and 0.1 mM GTP. After centrifugation, the supernatant was passed through glutathione-Sepharose™ 4B (Amersham Biosciences) column and washed with buffer N-100 plus 1 mM DTT. eIF4E and the mutants were eluted from the column after thrombin (Amersham Biosciences) digestion and further purified by Ultrogel AcA 44 gel filtration. All proteins were quantified by Bradford protein assay (46). The binding ability of eIF4E and mutants were tested by applying protein samples to a 7-methyl GTP-Sepharose 4B column essentially as described before (47). The column was then washed with ten volumes of N-100 buffer. Virtually the same volumes of (i) total protein prior to column binding, (ii) protein bound to the column resin, and (iii) unbound eluate were sampled and monitored by PAGE.

Protein RNA Interaction by Filter Binding—Filter binding assays were employed as described previously (35, 48) with slight modification. Nitrocellulose membrane was presoaked for 10 min in 0.4 M KOH followed by rinsing in nuclease free water to bring the pH to neutral. 0.02 pmol of [α-^{32}P]CTP-labeled RNA in 30 μl of binding buffer (100 mM KCl, 5 mM Mg$(CH_3COO)_2$, 1 mM DTT, 170 μg/ml bovine serum albumin, 170 ng/ml poly(dI-dC), 30 μg/ml tRNA, 10% glycerol, and 40 units/ml RNasin) was mixed with 20 μl of N-100 containing protein factors. The reaction was incubated at room temperature for 15 min and filtered through nitrocellulose and Hybond N++ nylon membranes (Amersham Biosciences), which were presoaked in washing buffer (25 mM HEPES-KOH, pH 7.6, 100 mM KCl, 4 mM $MgCl_2$, 1 mM DTT, and 10% glycerol), the membranes were then washed with 3 × 100 μl washing buffer. Both membranes were dried and exposed to a PhosphorImager screen. The bound RNA with protein, in complexes (retained on nitrocellulose) and free RNA (retained on Hybond N++ membrane), was calculated from the intensity of individual spot on the membranes with ImageQuant (Molecular Dynamics) or Quantity One (Bio-Rad) software. Each sample was measured in triplicate, and the data were obtained from three experiments.

RESULTS

The 3′-UTR of PEMV RNA 2 Is Required for Cap-independent Translation Initiation and Ribosomal Frameshifting—Nothing is known about cap-independent translation of umbraviruses. Thus, we set out to identify a CITE in PEMV RNA 2. Based on the very short 5′-UTR, long 3′-UTR, and genome similarity to luteo- and dianthoviruses, which harbor CITEs in their 3′-UTRs, we focused first on the 3′-UTR. Initially, we tested translation efficiencies of PEMV RNA 2 transcripts containing deletions in the 3′-end of the genome. Capped and uncapped RNAs were transcribed from the full-length clone, pPER2, after linearization with $SmaI_{4252}$, $SacII_{3576}$, or $HpaI_{1100}$ (subscripts indicate position of restriction site in the viral genome) and translated in wheat germ extract. The amount of ORF1 translation product (P1) from uncapped full-length RNA 2 (from $SmaI_{4252}$-linearized pPER2) was 81% of that obtained with the capped transcript, whereas RNAs with larger deletions trans-

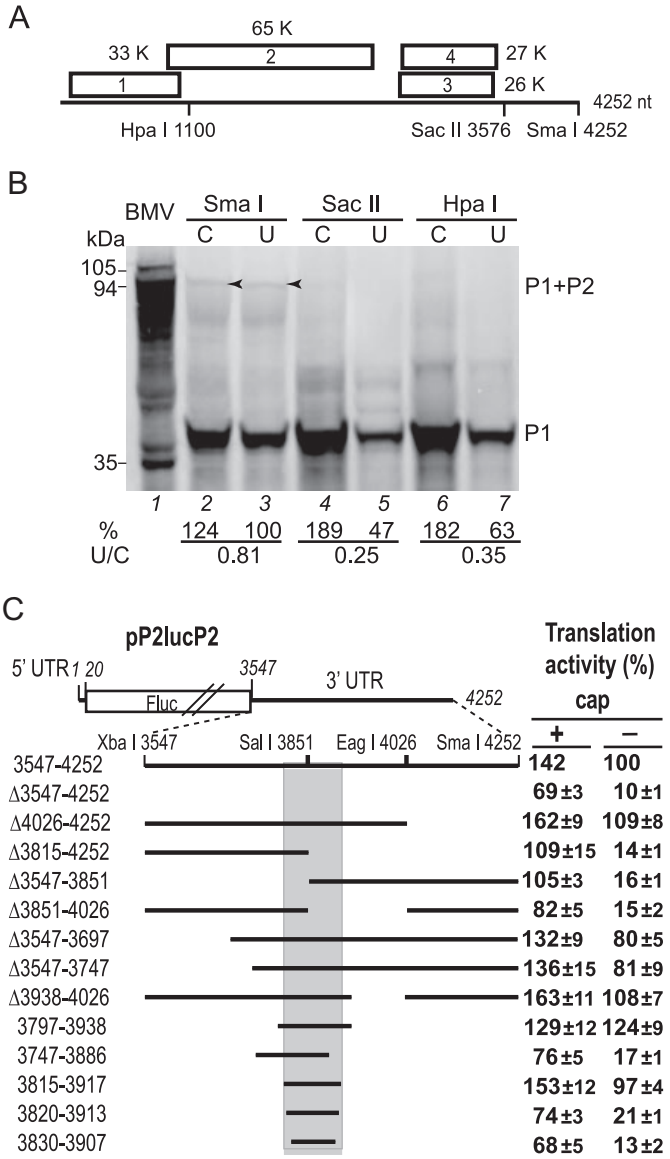

FIGURE 1. **Mapping the sequence in the PEMV RNA 2 3′-UTR required for cap independent translation.** *A*, genome organization of PEMV RNA 2. Positions of key restriction enzyme sites are indicated. *B*, translation of capped (*C*) or uncapped (*U*) transcripts from pPER2 linearized at the indicated restriction sites. The prominent band (*P1*) is the expected 33-kDa product of ORF1. The *faint band* indicated by *arrowheads* in *lanes 2* and *3* migrates as the predicted 94-kDa RNA-dependent RNA polymerase from the fusion of ORF1 and ORF2 by frameshift (*P1*+*P2*). Molecular weights of the protein products of BMV RNAs 1, 2, and 3 used as mobility markers are shown at the *left*. The relative amounts of ORF1 products (%) and the ratios of ORF1 products from uncapped/capped RNAs (*U/C*) are indicated below each pair of *lanes*. *C*, mapping the PTE. Map of P2lucP2 containing the full PEMV RNA2 UTRs flanking the firefly luciferase ORF (*Fluc*). *Black bars* below indicate portions of the 3′-UTR in the P2lucP2 deletion mutants listed at the *left*. Relative translation activities of capped (+) or uncapped (−) transcripts in wheat germ extract are shown in columns at the *right*. Translation activity is shown as the percentage of relative light units of those obtained from the uncapped P2lucP2 RNA (transcript with full-length PEMV RNA 2 UTRs) after 60 min. Data are averages (±S.D.) from at least three independent experiments. Deletion mutants were named either by the bases deleted from the 3′-UTR (indicated by △), or by the sequence remaining in the 3′-UTR (*left*). The sequence spanning nt 3815–3917 (*shaded rectangle*) was identified as the minimal PEMV RNA 2 translation element (PTE) necessary and sufficient for cap-independent translation.

lated only one-fourth to one-third as efficiently as their capped counterparts (Fig. 1*B*). It is clear that removal of a sequence downstream of base 3576 reduces translation of uncapped RNA by 65–75%, indicating that the PEMV 3′-UTR participates in translation of uncapped genomic RNA.

We also observed a very faint band of ~94 kDa in the products of full-length PEMV RNA2 (*arrowheads*, Fig. 1*B*). This product is the size predicted if ORF1 and ORF2 are translationally fused by −1 ribosomal frameshifting as predicted (38). Consistent with this prediction, the 94-kDa band is absent from the $HpaI_{1100}$ transcript, which lacks most of ORF2. Interestingly, no 94-kDa product was translated from the $SacII_{3576}$-linearized transcript even though it encodes the complete ORF2. These results indicate the requirement for a cis-acting signal downstream of $SacII_{3576}$ for frameshifting. This supports the prediction that a *cis*-acting element between bases 3612 and 3630 is necessary for frameshifting by long distance base pairing to a predicted stem-loop near the frameshift site (36), as is the case for *Luteovirus* RNAs (49).

To map the cap-independent translation element(s) precisely, a luciferase reporter construct was made by replacing the coding and intergenic regions of PEMV RNA 2 with the firefly luciferase coding sequence (construct pP2lucP2). RNA transcripts with numerous deletions in the 3′-UTR were translated in wheat germ extract. Relative translation efficiency was determined by comparing relative light units generated by the luciferase translated from the mutant reporter RNA with the relative light units generated from the wild-type RNA (P2lucP2). Uncapped RNAs containing 3′-UTR deletions limited to regions upstream of nt 3815 or downstream of nt 3917 were translated at least 80% as efficiently as uncapped full-length RNA (Fig. 1*C*). Addition of a 5′ cap-stimulated translation of these deletion mutants by no more than ~1.6-fold. Precise deletion mapping revealed that the sequence between bases 3815 and 3917 was necessary and sufficient for full cap-independent translation (Fig. 1*C*). We define this region as the PEMV RNA 2 cap-independent translation element (PTE).

Solution Probing of PTE RNA Secondary Structure—We next determined the secondary structure of the PTE by computer prediction, combined with structure-sensitive chemical modification and enzymatic digestion. The modification and cleavage sites in the PTE were identified by primer extension and denaturing gel electrophoresis. A transcript comprising viral sequence from nt 3777 to 3982 ($PTE_{3777-3982}$) was used for solution structure probing. A secondary structure of this sequence predicted using MFOLD (43) is shown in Fig. 2*A*. We ensured that this RNA was functional by employing a *trans*-inhibition assay similar to that which was used previously to define the BTE (35, 50). Increasing amounts of the $PTE_{3777-3982}$ were added in *trans* to a reaction containing P2lucP2 mRNA. A 25:1 ratio of $PTE_{3777-3982}$ to P2lucP2 RNA inhibited P2lucP2 translation to <20%, and a 50:1 ratio reduced translation to near-background levels (Fig. 2*B*). The slightly smaller minimal element defined in the above deletion experiments (Fig. 1*C*), $PTE_{3815-3917}$, inhibited translation with slightly less efficiency (Fig. 2*B*). As a negative control, we tested *trans*-inhibition activity of mutant PTEm2, which differs from wild-type PTE by two point mutations: C3868A and C3869A (Fig. 2*A*). PTEm2 does not stimulate cap-independent translation in *cis* (below). Unlike the wild-type PTE, PTEm2 did not inhibit translation in *trans* (Fig. 2*B*). Hence only a functional PTE inhibits trans-

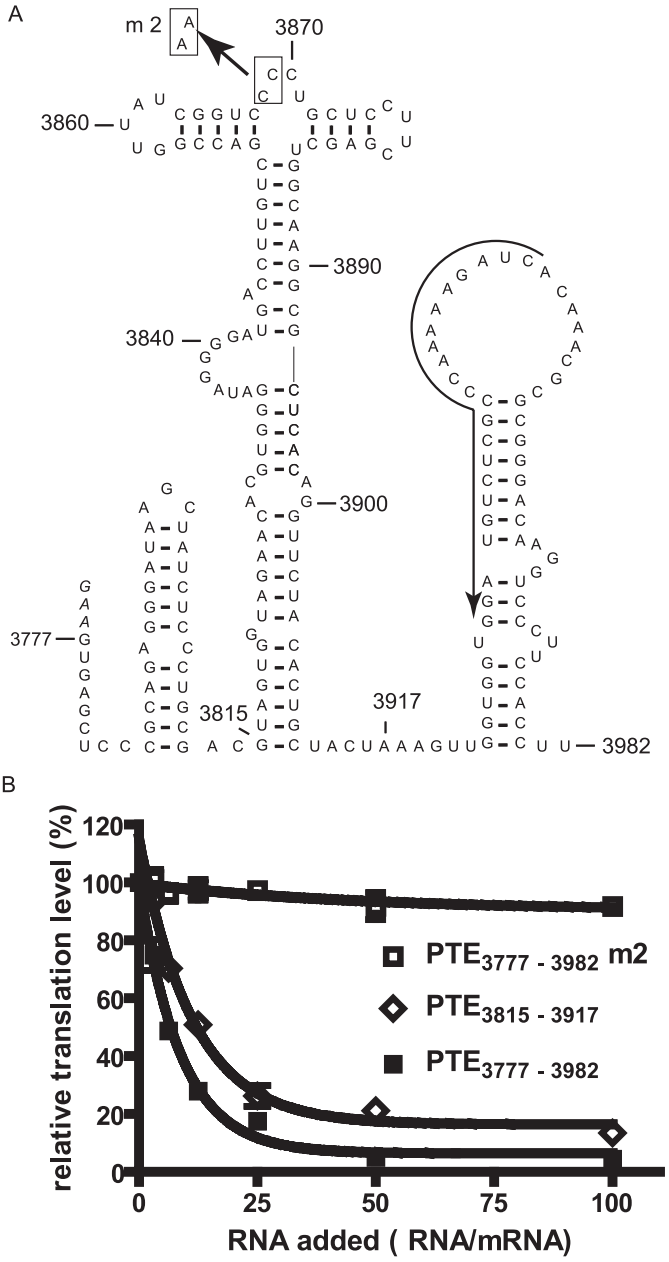

FIGURE 2. **Functional analysis by *trans* inhibition assay of the minimal functional RNA segment for solution structure probing.** *A*, predicted secondary structure of the RNA segment used for solution structure probing. The *arrow* along the sequence indicates the sequences to which ^{32}P-labeled oligomer was annealed for primer extension. *Boxed bases* were mutated to AA (*arrow*) in nonfunctional mutant PTEm2 (*m2*). Three non-viral bases, GAA (*italics*), were added to the 5′-end for efficient transcription by SP6 RNA polymerase. *B*, relative translation levels of P2lucP2 programmed wheat germ extract with increasing amounts of RNAs added in *trans*. Subscript indicates ends of the sequence of the *trans*-inhibiting RNA (*numbered* as in *panel A*). Relative translation is defined as 100% for the relative light units obtained in the absence of added PTE fragment.

lation in *trans* at these concentrations, confirming that the $PTE_{3777-3982}$ fragment is a biologically relevant substrate for RNA structure probing.

To probe the PTE RNA in solution we used the selective 2′-hydroxyl acylation analyzed by primer extension (SHAPE) protocol reagent NMIA, which acylates the 2′-hydroxyl moiety on exposed (usually single-stranded) nucleotides, in a sequence-independent manner (41, 42). We also employed RNase ONE, which cleaves all unpaired nucleotides. Modified bases were detected by primer extension (Fig. 3, *A–D*). The level of modification or cleavage at each base was superimposed on a best fitting predicted secondary structure, which consists of a long bulged helix bifurcating into two stem-loops (Fig. 3*E*). This structure agrees well with the solution probing data, except for two subdomains. The CCCU track (C domain) at the top of the three-way junction was predicted to be single-stranded but gave only a very weak signal in solution probing (C domain indicated in Fig. 3, *A* and *C*). In the predicted large G-rich-bulge loop (G domain) between helices H2 and H3, G3840 was modified by NMIA more strongly than the other bases in the G domain, and they were cleaved only weakly by RNase ONE (G domain, Fig. 3, *A* and *C*).

For comparison, the nonfunctional mutant PTEm2 (Fig. 2*A*) was also probed in solution. Interestingly, the two C-to-A mutations in the C domain rendered the C domain more accessible to NMIA and RNase ONE (Fig. 3, *D* and *F*). Unexpectedly, these two mutations also caused increased cleavage of the G domain bases by RNase ONE, giving a pattern predicted for a single-stranded G domain bulge. NMIA modification of the G domain also increased in m2, with the striking exception of G3840, which was less modified than in the wild-type PTE. The m2 mutations also caused nucleotides C3852 and U3884 (located opposite the C domain in the three-way junction) and G3893 (opposite the G domain) to become more extensively modified by NMIA (Fig. 3, *D* and *F*). No other substantial differences were observed in PTEm2.

The predicted structure of another translation enhancer element identified in panicum mosaic virus (PMV) (51) resembles the PTE element as follows: (i) both can be depicted as a T-shaped secondary structure with a long bulged helix featuring a large G-rich bulge on the 5′ side topped by seven consecutive base pairs (H3, Fig. 3, *E* and *G*), (ii) the top of the "T" branches into two stem-loops containing 5 (SL1) and 4 (SL2) bp, respectively, (iii) the loop of SL1 has potential to base pair to the 5′-UTR (below), (iv) the bulge connecting SL1 and SL2 is 4 bases long with a CCC tract, and (v) an unpaired U is conserved at the junction of SL2 and H3. There is no other obvious sequence similarity between the two elements, suggesting the G and C domains are important for PTE function. The conservation of secondary structure between the two viral RNAs provides phylogenetic support of the secondary structure determined experimentally.

Secondary Structure but Not the Sequence of the Branching Stem-loops Is Necessary for PTE Activity—To define the primary and secondary structures required for PTE function, mutations were introduced into the PTE of luciferase reporter construct pP2lucP2 containing the full-length 3′-UTR, and the resulting RNA transcripts were translated in wheat germ extract (Fig. 4*A*). Many were also translated in oat protoplasts (Fig. 4*B*).

Mutations that partially disrupted either helix of SL1 or SL2 (m7, m8, m21, and m22) brought down the translation activity to less than one-fourth of the wild-type level (Fig. 4*A*), whereas two other mutations predicted to restore SL1 (m23) or SL2 (m24) retained greater than three-fourths of wild-type activity

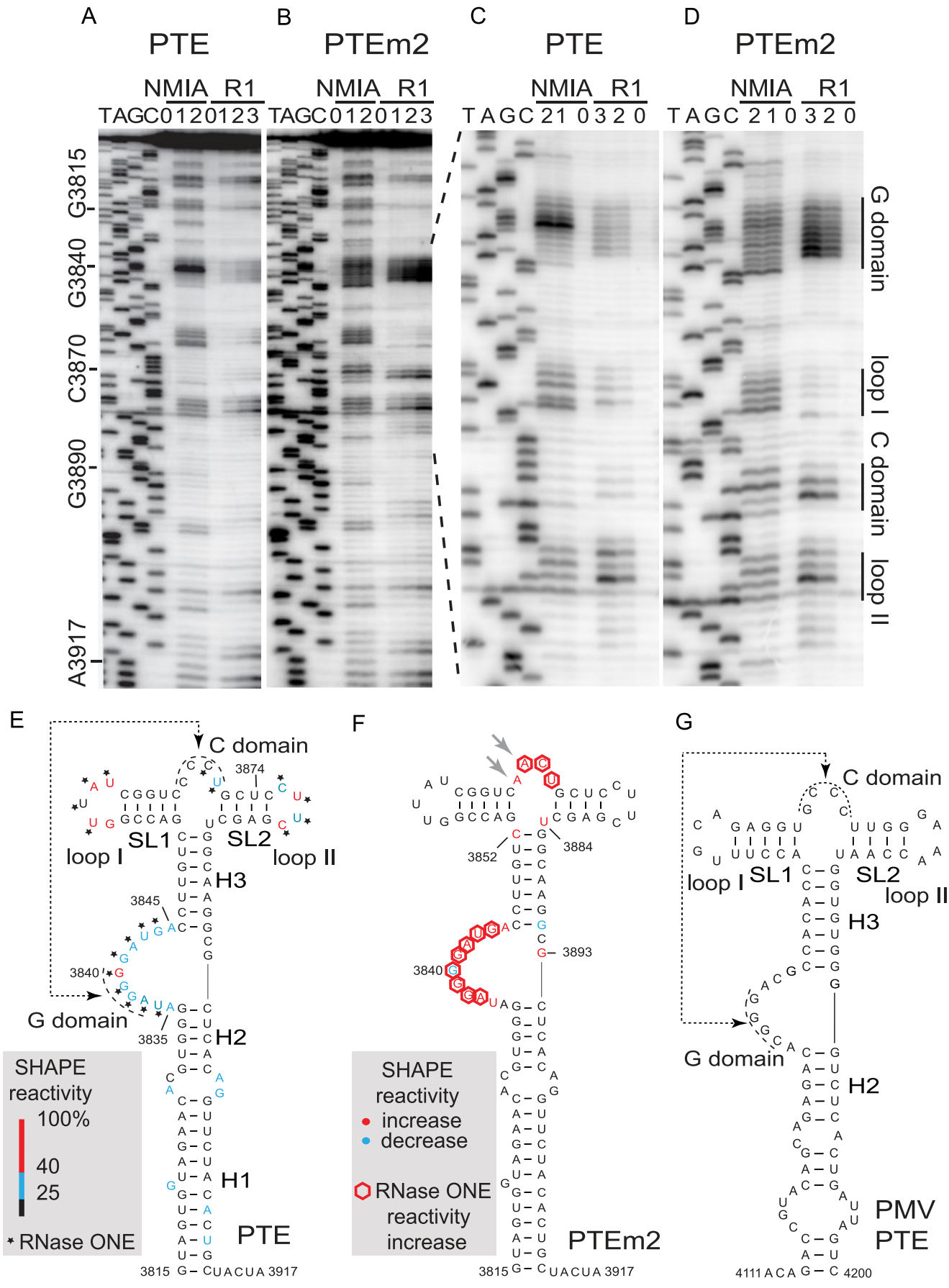
A
PTE
B
PTEm2
C
PTE
D
PTEm2
NMIA R1
TAGC0120123
TAGC21 0320
TAGC 210 320
G3815
G3840
C3870
G3890
A3917
G domain
loop I
C domain
loop II
E
C domain
SL1
SL2
loop I
loop II
H3
H2
H1
G domain
PTE
SHAPE reactivity
100%
40
25
RNase ONE
F
increase
decrease
RNase ONE reactivity increase
PTEm2
G
PMV PTE

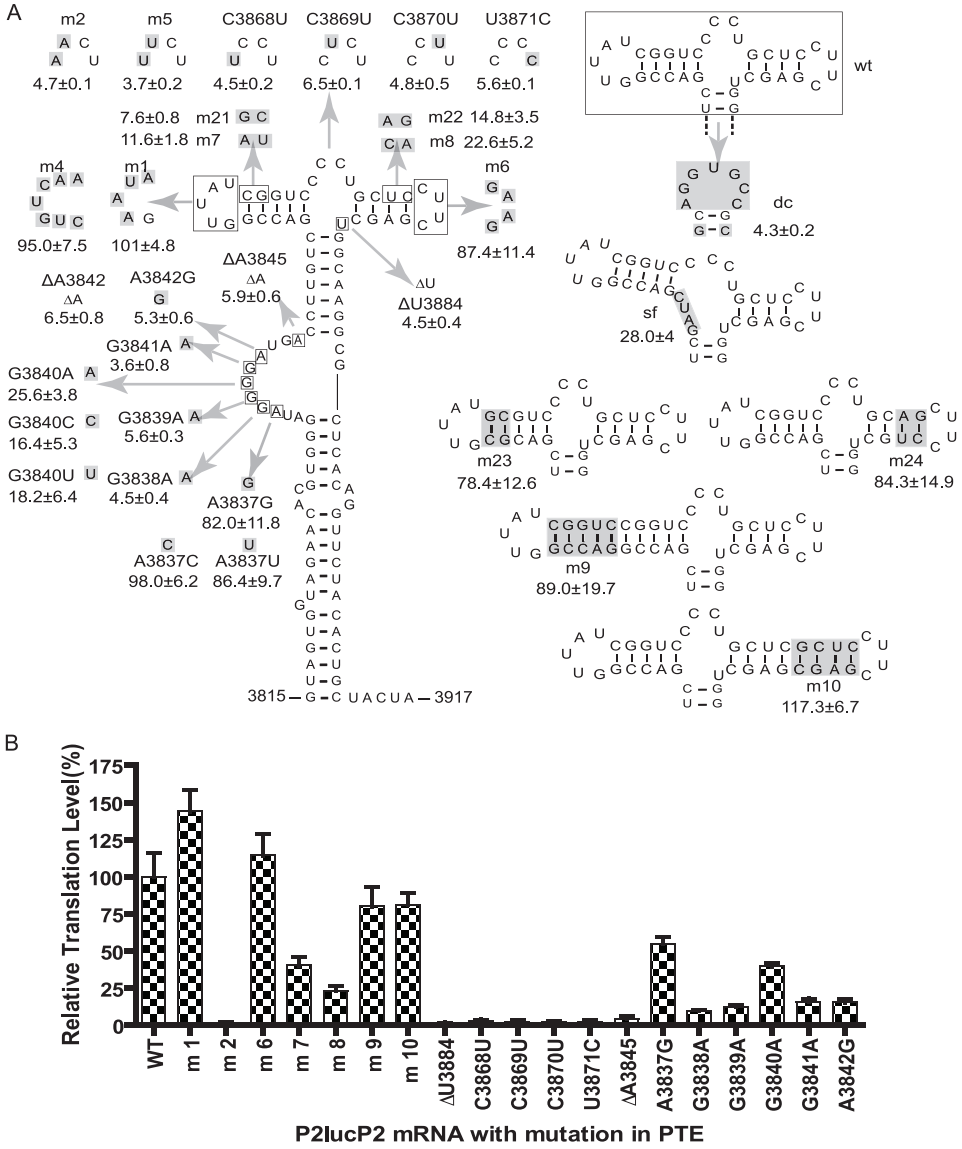

FIGURE 4. **Effects of mutations in the PTE on cap-independent translation *in vitro* and *in vivo*.** *A*, mutations introduced in PTE region (nt 3815–3917) in P2lucP2 are *shaded*. *Boxes* indicate groups of mutated bases. △, deletion. Major mutations to the *top portion* of the structure (*boxed*) are shown at *right*. *Numbers* below each construct indicate relative translation activity (mean ± S.D.) in wheat germ extract of uncapped mRNAs containing the indicated mutations in the P2lucP2 parent transcript. Relative translation is the percent of relative light units obtained from uncapped, wild-type P2lucP2 transcript. *B*, *bar graph* comparing relative luciferase levels obtained in oat protoplasts from P2lucP2-derived constructs containing the PTE mutations shown in *panel A*. Relative translation is defined as in *panel A*. See "Experimental Procedures" for details.

(Fig. 4*A*). Duplications that doubled the length of SL1 or SL2 (m9 and m10) retained near-wild-type translation activity.

Loop 1 has potential to base pair with the 5′-UTR in a long distance interaction similar to that required by some other 3′-UTR CITEs (52). However, mutations in loop 1 (m1 and m4) did not affect translation efficiency, and mutations in loop 2 (m6) also retained full activity. Thus, in the translation conditions used here, long distance base pairing between the PTE and 5′-UTR appears to be unnecessary. In summary, these data reveal that the branching stem-loops are necessary, but the sequences and lengths of these helices are not important for PTE activity. Structure probing of functional mutants m1, m6, m9, and m10 revealed that all retained the expected wild-type-like PTE structure (supplemental Fig. S1), confirming the structure is the determinant for PTE function.

Interaction of the C and G Domains Is Essential for Translation Activity—The role of unpaired bases around the helical junction was investigated in detail. All six constructs containing mutations in the C domain (m2, m5, C3868U, C3869U, C3870U, and U3871C) reduced translation of luciferase to background levels (~5% of wild-type) in wheat germ extract (Fig. 4*A*). Deletion of the unpaired U3884 connecting SL2 to H3 (ΔU3884) also abolished PTE translation activity. On the other hand, a four-base insertion (GAUC) between H3 and SL1 (mutant sf) allowed reduced, but significant (28.0%), translation in wheat germ extract (Fig. 4*A*). Single base deletions or substitutions of G3838, G3839, G3841, A3842, or A3845 in the G domain abolished translation activity. In contrast, mutations of A3837 retained near wild-type activities and mutations of the highly modification-sensitive G3840 retained significantly higher activities (16–26% of wild-type), than the mutations in the four surrounding sites (Fig. 4*A*).

The translation efficiencies of the selected mutant PTE constructs in oat protoplasts (Fig. 4*B*) were strikingly similar to the behavior of these RNAs in the wheat germ extract. This sup-

FIGURE 3. **Chemical and enzymatic solution structure probing of PTE and PTE m2 RNAs.** *A–D*, primer extension products from RNAs modified with NMIA or digested with RNaseONE (*R1*). PTE RNA (*A* and *C*) and PTE m2 RNA (*B* and *D*) were modified with NMIA (*1*, 60 mM; *2*, 120 mM) or digested with RNaseONE (1, 0.025 unit; 2, 0.05 unit; 3, 0.1 unit). "*0*" indicates no reagent control. *C* and *D*, gels were run longer to improve resolution of bases detected in the central portions (*dashed lines*) of gels in *panels A* and *B*, respectively. Positions of modified bases or RNase ONE cleavage sites were revealed by primer extension and bands were separated in an 8% polyacrylamide, 7 M urea sequencing gel. The sequencing ladders (*lanes TAGC*) were generated by dideoxy sequencing of the RNA with the same 5′-labeled primer used in the modification lanes. *E*, superposition of probe activities on the best-fitting predicted secondary structure of the PTE. SHAPE activity (level of NMIA modification) is indicated by color-coded bases. Possible pseudoknot interaction between G and C domain is indicated by *dashed double-headed arrow*. *F*, changes in modification or cleavage sensitivity of bases in PTEm2 compared with wild-type PTE. *G*, predicted secondary structure of the translation enhancer element of PMV, including the possible G–C domain pseudoknot.

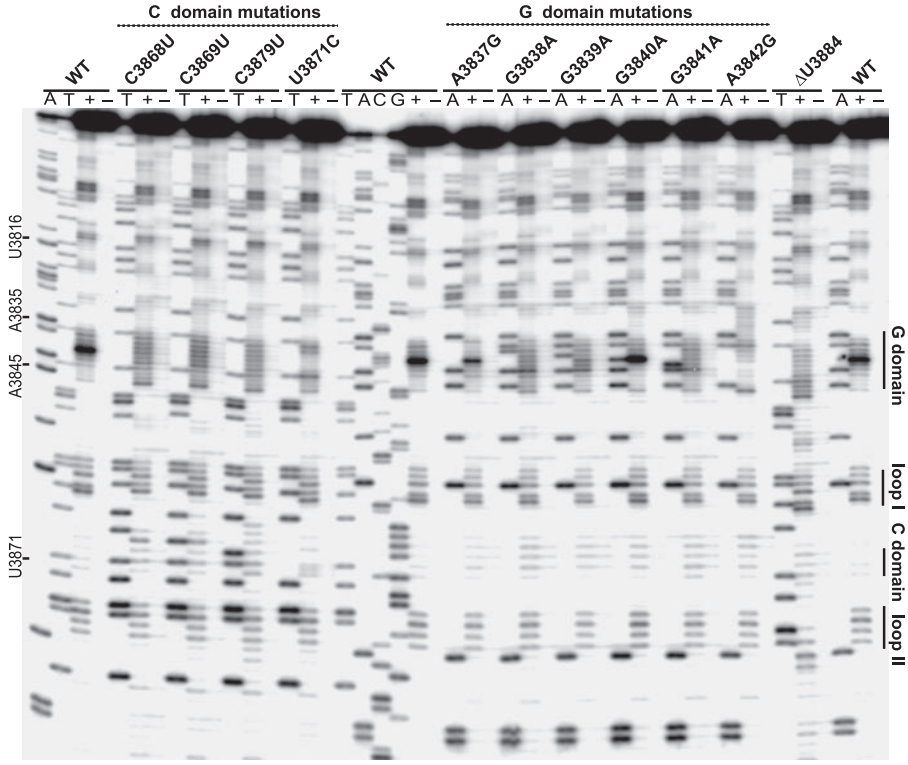

FIGURE 5. **SHAPE analysis of the PTE solution structure with mutations in the G and C domains.** RNA was modified with either 60 mM NMIA (+) or no reagent (−). The modified bases were revealed by primer extension as in Fig. 3. The sequencing ladders (*lanes TACG* beside wild-type RNA, and *T* or *A* beside each mutant) were generated by dideoxy sequencing of the RNA with same 5′-labeled primer used in the modification *lanes*.

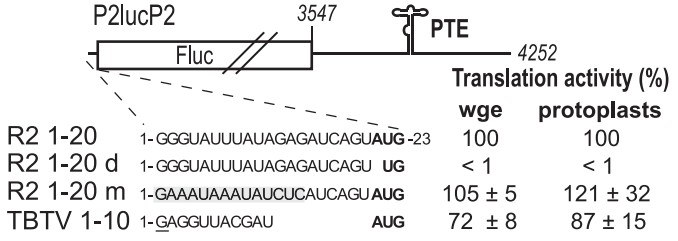

FIGURE 6. **Effects of mutations in the 5′-UTR on cap-independent translation of RNA containing the PTE in the 3′-UTR.** Mutations were introduced into the 5′-UTR of P2lucP2, and the corresponding uncapped mRNAs were translated in wheat germ extract and in oat protoplasts. Only bases up to and including the firefly luciferase ORF start codon (*bold*) are shown. *R2 1–20*: wild-type PEMV RNA 2 5′-UTR sequence (P2lucP2). *R2 1–20d*: adenosine in the start codon deleted. *R2 1–20m*: nt 2 and 3 (GG) mutated to AA, and nt 4–14 mutated to their complementary counterparts (*shaded*). *TBTV 1–10*: entire 10-nt TBTV 5′-UTR (GenBank™ accession no. AF402620), preceded by a non-viral extra G (*underlined*) for efficient RNA transcription. Relative translation efficiencies are shown as percentage of relative light units obtained with P2lucP2. Luciferase was measured after 1 h of translation in wheat germ extract (*wge*) or 4 h post electroporation in oat protoplasts.

ports the validity of the wheat germ extract as a system to analyze PTE translation.

Taken together, sequences in the C and G domains are critical for PTE translation activity, whereas the sequences of the predicted helices and loops I and II are not important, as long as their secondary structure is maintained. For these reasons we investigated the structure of selected G domain and C domain mutants in more detail by probing these mutants (as well as the ΔU3834 mutant) with NMIA. All nonfunctional mutations in either the C or G domains caused both domains to become more reactive to NMIA (Figs. 3*B*, 3*D*, and 5). The C domain is not strongly modified in the G domain mutants, but it is clearly modified more than in wild-type PTE RNA. In contrast, the rest of the structure remained unchanged in the C and G domain mutants. Nonfunctional G3838A, G3841A mutants were also probed by RNase ONE and, like PTEm2, both G and C domains were more accessible than wild-type (supplemental Fig. S2). These results indicate that elimination of translation activity was due to disruption of an interaction between the C and G domains.

We hypothesize that, in the wild-type PTE, the G and C domains interact to form a pseudoknot (*dashed arrow*, Fig. 3*E*), protecting both domains from the single strand-specific probes, with the exception of G3840. This tertiary interaction may be weak or dynamic, because nucleotides in the G and C domains are partially accessible to the probes. The extremely modifiable G3840 either does not participate in the pseudoknot base pairing, or it is base paired but arranged in such a way to make its 2′-hydroxyl highly exposed to NMIA. The mutations in the C or the G domain would eliminate the pseudoknot interaction, making nucleotides in both G and C domains single-stranded and more accessible to modification and cleavage, as observed (except for G3840, which becomes less, but still significantly, modified by NMIA in C domain mutants).

To test whether base pairing (and not sequence) between the C and G domains was sufficient to form a functional pseudoknot, seven different double mutants of P2lucP2 were tested with individual base pairs exchanged, to maintain the predicted C domain-G domain base pairing. None of these double mutants facilitated cap-independent translation (supplemental Fig. S3). We conclude that the sequences of the G and especially C domains are critical for PTE activity.

The 3′ PTE Mediates Translation Independent of Sequence in the 5′-UTR—Some viral 5′-UTRs participate in translation by recruitment of initiation factor(s), either directly (53, 54) or by interaction with the 3′-UTR (18, 52). To determine the role, if any, of the 20-nt PEMV RNA 2 5′-UTR in cap-independent translation, P2lucP2 mutants with alterations in the 5′-UTR were translated in wheat germ extract and in protoplasts (Fig. 6). As a negative control, deletion of the adenosine in the start codon was found to totally abolish translation. The RNA reporter with the first 14 nt in the 5′-UTR altered to their complementary sequences translated virtually the same as wild-type P2lucP2. Substituting the P2lucP2 5′-UTR with the even shorter 10-nt 5′-UTR from TBTV (another umbravirus)

slightly reduced translation efficiency. These data showed that no specific sequence in the 5′-UTR appears to be required for cap-independent translation mediated by the PTE in the 3′-UTR. They support the conclusion from mutations in loop 1 of the PTE (*m1* and *m4*, Fig. 4) that no base pairing between the PTE and the 5′-UTR is necessary for cap-independent translation under the conditions tested.

PTE Interacts with Translation Initiation Factor eIF4F but Not eIFiso4F—Binding of eIF4F (or eIFiso4F in plants) (55, 56) to the cap structure on the 5′-end of cellular mRNA is an important regulatory step in eukaryotic mRNA translation initiation (1, 5, 57). This leads to ribosome recruitment followed by scanning for the initiation codon (58–60). As described above, PTE stimulates translation in *cis* (Fig. 1) and inhibits translation in *trans* (Fig. 2*B*). We hypothesize that this behavior is due to interaction of the PTE with translation initiation factor(s) and that this interaction competes with the mRNA for essential factors needed to recruit the ribosome. This was shown to be the case for the BTE of BYDV (35). To test this possibility with the PTE, we first inhibited translation in a wheat germ extract by adding excess PTE RNA in *trans*, then we observed the effects of adding increasing amounts of exogenous initiation factors on translation of P2lucP2. Indeed, the *trans* inhibition was reversed, and translation of P2lucP2 was recovered fully by addition of ~100 nM eIF4F (Fig. 7*A*). eIFiso4F was far less stimulatory and did not restore full translation. Addition of eIF4F or eIFiso4F both stimulated translation of the uninhibited extract by ~40% in the presence of 200 nM added factor (Fig. 7). These results indicate that *trans* inhibition is specific to sequestration of eIF4F, not eIFiso4F, and both factor complexes are somewhat limiting in uninhibited wheat germ extract.

To determine if the stimulation of PTE-mediated translation is due to direct PTE binding by eIF4F, we performed a filter binding assay of the PTE with eIF4F or eIFiso4F. The PTE (nt 3815–3917) bound eIF4F with high affinity (K_d = 48 nM) (Fig. 8*A* and Table 1). The non-functional mutant, PTEm2 (Fig. 4*A*), did not bind eIF4F (Fig. 8*A*), indicating that PTE function correlates with its affinity for eIF4F. Wild-type PTE did not bind significantly to eIFiso4F (Fig. 8*B*). As a positive control for eIFiso4F binding, we measured eIFiso4F binding to the TED (nt 621–752) in the 3′-UTR of STNV-1 RNA, which had been shown previously to bind eIFiso4F (32). Up to 50% of STNV-1 TED was bound by 500 nM eIFiso4F. In contrast, only 15% of PTE was bound at this concentration (Fig. 8*B*). In summary, the factor binding data as well as translation recovery data indicate that eIF4F rather than eIFiso4F interacts directly with PTE to facilitate cap-independent translation.

PTE Interacts with eIF4F Via the eIF4E Subunit—We next sought to determine which of the eIF4F subunits, eIF4E or eIF4G or both, binds directly to the PTE. For the filter binding assay both proteins were purified using improvements to the existing protocols (44). Switching from the previously published pET3d expression vector (44) to pET28a (Novagen) increased the expression in *E. coli* at least 3-fold. Because most degradation occurs in the N-terminal region of eIF4G, we fused a His_6 tag to the N terminus and purified eIF4G by immobilized metal affinity chromatography, followed by gel filtration. eIF4E and mutants were purified as a GST-tagged fusion protein. Using factors purified by these methods (Fig. 8*C*), the PTE was found to bind eIF4E with a much higher affinity (K_d = 58 nM) than eIF4G (K_d > 800 nM) (Fig. 8*D* and Table 1).

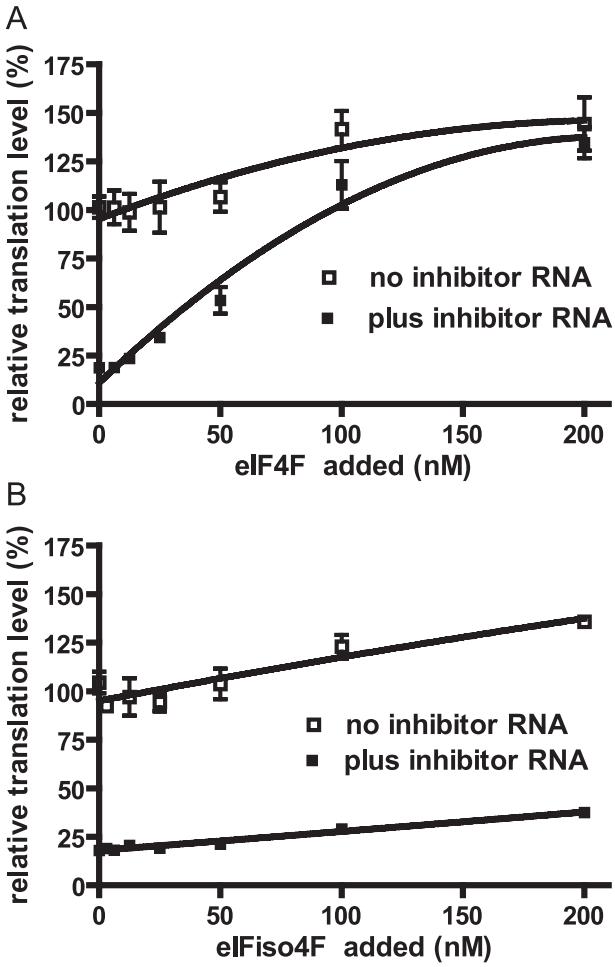

FIGURE 7. **Effect of adding eIF4F or eIFiso4F to PTE-inhibited wheat germ translation extract.** Each reaction contained 4 nM P2lucP2 RNA in 50 μl of wheat germ extract. Forty-fold excess (160 nM) $PTE_{3815–3917}$ was present in the reactions indicated by *solid squares* (plus inhibitor RNA). The amount of eIF4F or eIFiso4F added to the translation reaction is indicated on the *x*-axes. *Open squares* indicate translation levels obtained in the absence of *trans*-inhibiting $PTE_{3815–3917}$ RNA (no inhibitor RNA). Relative translation efficiencies are shown as percentage of relative light units obtained in 1 h in the absence of added *trans*-inhibitor RNA or factors.

eIF4E purified via GST tag (which was removed from the final preparation) bound a higher percentage of PTE RNA (~85%) at saturating levels than the preparation obtained by m^7GTP-Sepharose affinity chromatography (~70%). However, the K_d values measured from different experiments were similar (52–79 nM). The difference in maximum RNA binding may be due to residual m^7GTP, used in eluting eIF4E from the m^7GTP-Sepharose column, affecting the binding capacity of eIF4E for the PTE.

The specificity of the low affinity eIF4G binding to the PTE was investigated further. We found that 400 nM eIF4G bound the non-functional mutant PTEm2 with the same relative affinity as wild-type PTE: 29 ± 8%. A similar value was also observed for eIF4G binding to 18 S RNA, indicating that

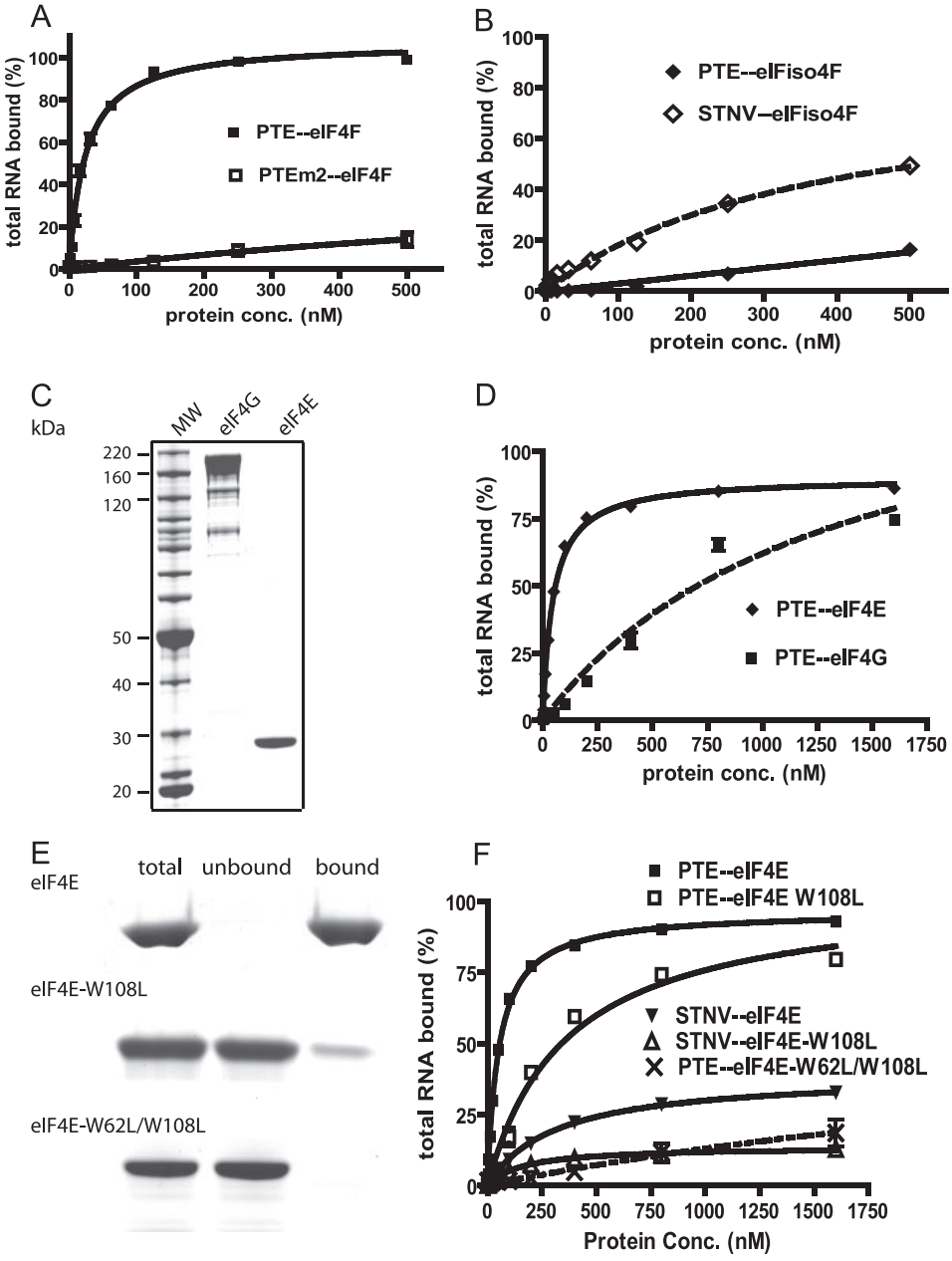

FIGURE 8. **Filter binding assays of translation initiation factors with the PTE or TED.** *A*, binding of $PTE_{3815–3917}$ and $PTE_{3815–3917}$ m2 to eIF4F. *B*, binding of $PTE_{3815–3917}$ and STNV-1 TED nt 621–752 (37) to eIFiso4F. *C*, PAGE of *E. coli*-expressed, purified eIF4G, and eIF4E ("Experimental Procedures") used in the filter binding assay in *panel D*. Mobilities (in kDa) of molecular mass markers are indicated at the *left* of *lane MW*. *D*, filter binding of $PTE_{3815–3917}$ to eIF4G or eIF4E. *E*, PAGE of wild-type and mutant eIF4E, purified as GST fusion proteins, which bound or flowed through (unbound) an m^7G-Sepharose column. The GST tag was removed after purification. *F*, filter binding of $PTE_{3815–3917}$ or STNV-1 TED nt 621–752 (37) to eIF4E or mutants. In each legend the RNA and protein that interact are separated by a *double dash*. For all filter binding assays in this figure, ^{32}P-RNA (~0.8 nM) was mixed with indicated concentration of protein and filtered onto layered nitrocellulose and nylon membranes to allow quantification of bound and unbound RNA, respectively ("Experimental Procedures"). The data are representative of at least three independent experiments.

binding of PTE to eIF4G is nonspecific. It occurs probably via the known nonspecific RNA-binding domains in eIF4G (10, 55, 59).

Because the PTE binds eIF4E so much more tightly than eIF4G, we tested whether eIF4E alone could restore translation in *trans*-inhibited extracts (as in Fig. 7). Adding up to 3 μM eIF4E had no effect on translation that remained at ~20% in the presence of 40× excess $PTE_{3815–3917}$ inhibitor. These results can be explained by the fact that eIF4E alone has no ability to stimulate translation directly, and that the key protein in recruiting factors and ribosomes, eIF4G, remains limiting and bound (in the form of eIF4F) to the excess *trans*-inhibiting PTE in these reactions.

The PTE Has a Higher Affinity than TED for eIF4E and a Different Requirement for the Cap-binding Pocket—The m^7GpppG cap structure on mRNA binds in the cap-binding pocket of eIF4E between two conserved tryptophan residues, which form π-π stacking interactions with the guanosine rings of the cap (3, 45, 61, 62). To explore whether eIF4E requires the cap-binding pocket to bind the PTE, we measured the binding affinity of two eIF4E mutants, eIF4E-W108L and eIF4E-W62L/W108L, in which one or both of the key tryptophan residues was altered to leucine. A single tryptophan mutation is known to prevent cap binding in murine eIF4E (47). In our hands, the single mutant, eIF4E-W108L, reduced but did not eliminate binding to 7-methyl GTP-Sepharose 4B (Fig. 8*E*). In contrast, the double tryptophan mutations in eIF4E-W62L/W108L abolished m^7GTP binding (Fig. 8*E*). eIF4E-W108L bound the PTE with about an 8-fold lower affinity (K_d = 461 nM) than wild-type eIF4E (K_d = 58 nM), whereas the double mutant, eIF4E-W62L/W108L, showed only background levels of binding and had no measurable K_d (Fig. 8*F*). Thus the ability of eIF4E and its mutants to bind m^7GTP generally correlated with their ability to bind the PTE. We conclude that interaction of eIF4E with PTE RNA requires an intact cap binding pocket.

Although STNV-1 TED is known to have eIF4E-binding activity (32), its dependence on the cap-binding pocket has not been determined. To address this, we measured the binding of TED to eIF4E-W108L. Disruption of the cap-binding pocket reduced the binding affinity (K_d) by at least 5-fold in all our experiments. Because the initial affinity of TED for eIF4E is low (much less than that of the PTE), and the limitation of filter binding to measure weak RNA-protein interaction, we could not obtain a meaningful K_d for the TED-eIF4E-W108L interaction. Given

that the PTE, but not the TED, showed significant binding to eIF4E-W108L, we conclude that the interaction between the PTE with eIF4E is different than the TED-eIF4E interaction. This is not surprising given the entirely different structures and sequences of these two RNA elements.

Binding of PTE Mutants to eIF4E Correlates Strongly with Their Ability to Stimulate Cap-independent Translation—To determine whether eIF4E binding affinity correlates with, and thus plays a role in, PTE-mediated cap-independent translation, we compared the binding affinities of several PTE mutants with their ability to facilitate cap-independent translation in the P2lucP2 context. To ensure that the relative binding observed was sensitive to changes in eIF4E-PTE affinity, the binding was measured at 100 nM eIF4E for all mutant RNAs tested. PTE mutants m1, m9, and A3837G all bound to eIF4E (Fig. 9) and conferred translation at similar level as wild-type PTE. All C domain mutants (m2, C3868U, C3869U, C3870U, and U3871C) and G domain mutants (G3838A, G3839A, G3841A, and A3842G) that abolished translation showed little or no binding to eIF4E (Fig. 9). Mutants m7, m8, and G3840A, which translated at low but significant levels, showed a proportionally reduced level of eIF4E binding. Slight deviations between eIF4E binding and translation stimulation activity were found in the SL2 of the PTE. Mutant m6 (SL2 loop sequence change) RNA bound eIF4E 50% more efficiently than wild-type RNA, but translated at wild-type levels; and mutant m10 (extension of the SL2 helix) bound eIF4E with only ~67% of wild-type affinity but translated with slightly higher than wild-type efficiency. Overall, the eIF4E binding capacities of the mutants correlated well with their ability to foster cap-independent translation in P2lucP2. We conclude that binding of PTE to the eIF4E subunit of eIF4F is necessary for cap-independent translation mediated by the PTE.

TABLE 1
Apparent dissociation constants of initiation factor-CITE interactions

Initiation factor	Estimated K_d		
	PTE[a]	STNV-TED	BTE[b]
		nM	
eIF4F	48 ± 21	17–30[c]	37 ± 8
eIF4E	58 ± 16	313[a] or ~780[c]	>2000
eIF4G	>800	ND[d]	177 ± 10

[a] Determined in this paper.
[b] Data from Ref. 35.
[c] Data from Ref. 32.
[d] ND, not determined.

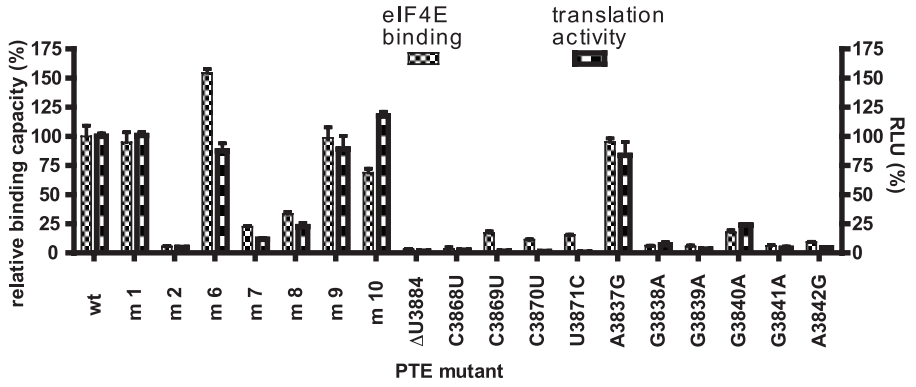

FIGURE 9. **Comparison of eIF4E binding and translation activities of PTE mutants.** Filter binding assays were performed as described in the Fig. 8 legend and under "Experimental Procedures" using 0.8 nM ^{32}P-RNA mixed with 100 nM eIF4E. The relative binding capacity (*left y axis*) is calculated by defining the percentage of total wild-type PTE bound to eIf4E as 100%. Relative translation (*right y axis*) is the percentage of relative light units obtained from each uncapped mutant transcript (Fig. 4*A*), relative to the wild-type P2lucP2 transcript.

DISCUSSION

The PTE Differs from other Cap-independent Translation Elements—Compared with previously published CITEs, the PTEs of PEMV RNA 2 and PMV RNA comprise a different structural class of element located in the 3′-UTR. The known 3′-UTR CITEs fall into about eight classes, each class defined by having a completely different secondary structure and sequence (13). The PTE class has only two known members, PEMV RNA 2 and PMV, a member of genus *Panicovirus* in the Tombusviridae family (Fig. 3, *E* and *G*). None of the other known or predicted elements form the same "T-shaped" structure with the probable pseudoknot interaction between the C and G domains (12, 13).

Interaction of the C and G domains is indicated by the observation that mutations in the C domain affect the accessibility of G domain and *vice versa*, whereas the predicted helical regions and terminal loops of the PTE remain unaffected by these base changes. A striking feature is that, in all functional mutants, base 3840 is highly susceptible to NMIA modification but not RNase cleavage (Figs. 3, 5, S1, and S2). The PTE functions to some extent with any base at this position, although it is most efficient with the wild-type G (Fig. 4*A*). Thus this base is likely unpaired. Various double mutations were introduced in attempts to maintain proposed base pairing between the C and G domains by various possible arrangements of complementary bases in these domains, but none were functional (supplemental Fig. S3). Therefore, although a pseudoknot is possible, other types of interactions between the C and G domains must be considered.

The PTE Facilitates Cap-independent Translation by Binding eIF4E—Several lines of evidence support a key role for eIF4E in the function of the PTE. In an analysis of eighteen different PTE mutants, eIF4E binding affinity correlated strongly with ability to facilitate cap-independent translation (Fig. 9). Moreover, the PTE alone, but not PTEm2, inhibited translation in *trans* (Fig. 3), and this inhibition was overcome by addition of eIF4F (but not eIFiso4F) to the translation extract (Fig. 7*A*). Thus it appears that the PTE recruits eIF4F by binding the eIF4E subunit of eIF4F even though the PTE lacks the m^7GpppN.

The PTE likely uses a non-standard interaction to bind eIF4E in the absence of a m^7G residue. The m^7G group forms crucial π bonds with specific tryptophan residues in the eIF4E cap-binding pocket (45). Mutation of one or both of the tryptophan residues reduced or eliminated, respectively, binding by PTE (Fig. 8*F*). Thus, it is clear that intact cap-binding pocket is necessary for PTE binding, but this does not prove that the PTE binds directly in

the cap-binding pocket. In the absence of a bound cap, the structure of eIF4E is less stable, and mutations of the cap-binding pocket may affect the overall structure of eIF4E (45, 63, 64). An uncapped RNA aptamer selected to bind mammalian eIF4E with high affinity bound the equivalent of the W108L eIF4E mutant (W102F in mouse eIF4E) with the same affinity as wild-type eIF4E (65). Thus, for the only other eIF4E-uncapped RNA interaction that we know of, a fully intact cap-binding pocket is not necessary.

PTE Differs from Other Plant Viral RNAs in Its Interactions with eIF4F Subunits—Other 3′ CITEs may interact with eIF4E. Genetic evidence indicates that the 3′ CITE of melon necrotic spot virus (MNSV, Tombusviridae), which does not resemble the PTE, also requires eIF4E (66). The direct factor binding of the MNSV CITE is unknown, but a natural point mutation (H228L) in melon eIF4E confers resistance to most MNSV strains, and this mutation prevents eIF4E from promoting MNSV CITE-mediated cap-independent translation *in vitro*. Moreover, a resistance-breaking mutant of MNSV had base changes in its CITE that allowed it to mediate cap-independent translation in the presence of the eIF4E-228L (67). Thus it is clear that the MNSV CITE relies on eIF4E for cap-independent translation, which is essential for infection. It will be interesting to see whether the MNSV CITE binds directly to eIF4E (or eIFiso4E) and, if so, how that interaction compares with the PTE-eIF4E mechanism.

Viruses in the large, diverse Potyviridae family may also facilitate cap-independent translation via eIF4E but by its interaction with the viral genome-linked protein (VPg) (26, 31, 68). This binding is required for infection (27, 29, 30), enhances viral RNA translation (28), and may inhibit host mRNA translation by sequestering eIF4E. Many natural potyvirus resistance genes in plants are mutant or deleted alleles of eIF4E or eIFiso4E (27, 69, 70). Potyviruses contain an IRES in the 5′-UTR (71), which binds and requires eIF4G (but not eIFiso4G) to facilitate cap-independent translation (10). Thus, potyviruses may recruit eIF4F by two routes: IRES binding of eIF4G and VPg binding of eIF4E.

The BTE of luteo-, diantho-, and other umbraviruses binds and requires eIF4G (35) and does not bind eIF4E, although eIF4E enhances BTE binding affinity by eIF4G and translation activation by ~30% (Table 1). This is likely because the activity of eIF4G is enhanced by binding of eIF4E even in cap-dependent translation (2). Unlike the binding of eIF4E to the PTE, binding of eIF4G to the BTE is less specific. A non-functional mutant of the BTE binds eIF4G with nearly the same affinity as does wild-type BTE, although completely unrelated RNAs bind eIF4G with lower affinity (35). In contrast, all of the functional PTE mutants, and none of the nonfunctional mutants, bind eIF4E (Fig. 9).

Another unrelated 3′ cap-independent translation element, the TED of STNV RNA, binds eIF4E but with substantially lower affinity than the PTE-eIF4E interaction (Table 1). TED also binds eIFiso4E (32). The TED binds eIF4F or eIFiso4F with much higher affinity than it binds any of the subunits (Table 1). As shown in Fig. 8*F*, both the TED and PTE require an intact cap-binding pocket to bind eIF4E, but the single W108L mutation has a greater negative effect on TED binding than on PTE binding.

In summary, where interactions with translation factors have been characterized, all 3′ CITEs bind the eIF4F complex with the highest affinity (Table 1). The PTE interacts via the eIF4E subunit of eIF4F, the BTE via the eIF4G subunit, and the TED of STNV prefers to bind the whole eIF4F heterodimer rather than primarily to a particular subunit. Thus, although the specific interactions with eIF4F differ among 3′ CITEs, the general mechanism of 3′ CITE function is the same: to recruit eIF4F. We speculate that each element has evolved to bind a different surface on the eIF4F complex.

Communication with the 5′-End of the Viral RNA—It is unclear how eIF4F, once bound by the PTE, is delivered to the 5′-end of PEMV RNA 2 where translation initiates. Almost all 3′ CITEs, including the PTE, have loop sequences predicted to base pair to the 5′-UTR (13, 18, 52, 72). For BYDV and TBSV, this base pairing is required for cap-independent translation (18, 52). Bases in loop 1 of SL1 in the PTE (3859UUAU3862) have potential to form weak base pairing to a sequence, 9AUAG12, in the 5′-UTR. Numerous alterations to loop 1, and to the 5′-UTR, did not affect PTE activity (Fig. 6). However, in some cases fortuitous base pairing between the mutant sequences can be predicted. For example, the AAUA sequence in m1 loop 1 may pair to a UUAU sequence in the 5′-UTR. This may explain the slightly higher than wild-type expression in protoplasts (Fig. 4*B*). Also, the reversed portion of the 5′-UTR in mutant 1–20m (Fig. 6) may pair to loop 1 via an AAUA-UUAU interaction. However, we predict no base pairing between the m4 loop 1 and the 5′-UTR or between the TBTV 5′-UTR and loop 1, yet these constructs also translate at near-wild-type levels. Thus, there appears to be no requirement for long distance base pairing between 5′- and 3′-UTR for PTE-mediated translation in the conditions used here. This resembles the TED sequence in which disruption of potential base pairing between the terminal loop of TED and the 5′-UTR only slightly reduced translation efficiency, and wild-type levels of translation were not restored by compensating mutations (73). Also, no base pairing of the 3′ CITE of Turnip crinkle virus to the 5′-UTR is apparent (74). Instead this tRNA-like structure binds the P site of 80 S ribosomes directly, and the 5′-UTR also plays a role in CITE activity (75). In contrast, in PEMV RNA2 and other umbraviruses, the 5′-UTR is so short (10–20 nt) that the ribosome may bind and interact with the start codon to some extent without eIF4 factors (16), and the 3′ PTE may simply enhance translation by increasing the local concentration of eIF4F.

Divergent Origins of Viral 3′ Cap-independent Translation Elements—It is intriguing that PEMV-2, in the *Umbravirus* genus (which is not assigned to a family), and PMV, the sole member of genus *Panicovirus* in the large, diverse Tombusviridae family, contain similar elements, while no other viruses are known to have a PTE. The two other sequenced umbraviruses contain a predicted BTE instead.[5] Other members of the Tombusviridae family, to which PMV belongs, have a variety of different CITEs (13, 18, 72–74, 76), and there is no correlation between the relationship of the viruses and the type of CITE each virus contains (13). Thus, as plant viruses evolve, they

either exchange *cis*-acting translational control signals, and/or different viruses may have independently evolved structures that recruit eIF4F. In some cases, such as PEMV RNA 2 and PMV, similar structures may have arisen by convergent evolution. Regardless of the evolutionary process, it appears that different classes of CITE act by different interactions to achieve the same result: recruiting the translational machinery.

Acknowledgments—We thank Karen Browning for providing cDNA clones of initiation factors, Aurélie Rakotondrafara and Jelena Kraft for valuable discussions, and Randy Beckett and Nikki Krueger for laboratory support.

REFERENCES

1. Gingras, A. C., Raught, B., and Sonenberg, N. (1999) *Annu. Rev. Biochem.* **68,** 913–963
2. Gross, J. D., Moerke, N. J., von der Haar, T., Lugovskoy, A. A., Sachs, A. B., McCarthy, J. E. G., and Wagner, G. (2003) *Cell* **115,** 739–750
3. Marcotrigiano, J., Gingras, A.-C., Sonenberg, N., and Burley, S. K. (1997) *Cell* **89,** 951–961
4. Pestova, T. V., Lorsch, J. R., and Hellen, C. U. (2007) in *Translational Control in Biology and Medicine* (Mathews, M. B., Sonenberg, N., and Hershey, J., eds) pp. 87–128, Cold Spring Harbor Laboratory Press, Cold Spring Harbor, NY
5. von der Haar, T., Gross, J. D., Wagner, G., and McCarthy, J. E. G. (2004) *Nat. Struct. Mol. Biol* **11,** 503–511
6. Amrani, N., Ghosh, S., Mangus, D. A., and Jacobson, A. (2008) *Nature* **453,** 1276–1280
7. Hentze, M. W., Gebauer, F., and Preiss, T. (2007) in *Translational Control in Biology and Medicine* (Mathews, M. B., Sonenberg, N., and Hershey, J., eds) pp. 269–295, Cold Spring Harbor Laboratory Press, Cold Spring Harbor, NY
8. Wells, S. E., Hillner, P. E., Vale, R. D., and Sachs, A. B. (1998) *Mol. Cell* **2,** 135–140
9. Browning, K. S. (1996) *Plant Mol. Biol.* **32,** 107–144
10. Gallie, D. R., and Browning, K. S. (2001) *J. Biol. Chem.* **276,** 36951–36960
11. Jan, E. (2006) *Virus Res.* **119,** 16–28
12. Kneller, E. L., Rakotondrafara, A. M., and Miller, W. A. (2006) *Virus Res.* **119,** 63–75
13. Miller, W. A., Wang, Z., and Treder, K. (2007) *Biochem. Soc. Trans.* **35,** 1629–1633
14. Goss, D. J., Carberry, S. E., Dever, T. E., Merrick, W. C., and Rhoads, R. E. (1990) *Biochemistry* **29,** 5008–5012
15. Kozak, M. (1991) *J. Biol. Chem.* **266,** 19867–19870
16. Pestova, T. V., and Kolupaeva, V. G. (2002) *Genes Dev.* **16,** 2906–2922
17. Rakotondrafara, A. M., Polacek, C., Harris, E., and Miller, W. A. (2006) *RNA* **12,** 1893–1906
18. Fabian, M. R., and White, K. A. (2004) *J. Biol. Chem.* **279,** 28862–28872
19. Karetnikov, A., and Lehto, K. (2007) *J. Gen. Virol.* **88,** 286–297
20. Mizumoto, H., Tatsuta, M., Kaido, M., Mise, K., and Okuno, T. (2003) *J. Virol.* **77,** 12113–12121
21. Timmer, R. T., Benkowski, L. A., Schodin, D., Lax, S. R., Metz, A. M., Ravel, J. M., and Browning, K. S. (1993) *J. Biol. Chem.* **268,** 9504–9510
22. van Lipzig, R., Gultyaev, A. P., Pleij, C. W., van Montagu, M., Cornelissen, M., and Meulewaeter, F. (2002) *RNA* **8,** 229–236
23. Fabian, M. R., and White, K. A. (2006) *RNA* **12,** 1304–1314
24. Wang, S., and Miller, W. A. (1995) *J. Biol. Chem.* **270,** 13446–13452
25. Ray, S., Yumak, H., Domashevskiy, A., Khan, M. A., Gallie, D. R., and Goss, D. J. (2006) *J. Biol. Chem.* **281,** 35826–35834
26. Beauchemin, C., Boutet, N., and Laliberte, J.-F. (2007) *J. Virol.* **81,** 775–782
27. Charron, C., Nicolaï, M., Gallois, J. L., Robaglia, C., Moury, B., Palloix, A., and Caranta, C. (2008) *Plant J.* **54,** 56–68
28. Khan, M. A., Miyoshi, H., Gallie, D. R., and Goss, D. J. (2008) *J. Biol. Chem.* **283,** 1340–1349
29. Lellis, A. D., Kasschau, K. D., Whitham, S. A., and Carrington, J. C. (2002) *Curr. Biol.* **12,** 1046–1051
30. Leonard, S., Plante, D., Wittmann, S., Daigneault, N., Fortin, M. G., and Laliberte, J.-F. (2000) *J. Virol.* **74,** 7730–7737
31. Wittmann, S., Chatel, H., Fortin, M. G., and Laliberté, J.-F. (1997) *Virology* **234,** 84–92
32. Gazo, B. M., Murphy, P., Gatchel, J. R., and Browning, K. S. (2004) *J. Biol. Chem.* **279,** 13584–13592
33. Guo, L., Allen, E., and Miller, W. A. (2000) *RNA* **6,** 1808–1820
34. Shen, R., and Miller, W. A. (2004) *J. Virol.* **78,** 4655–4664
35. Treder, K., Pettit Kneller, E. L., Allen, E. M., Wang, Z., Browning, K. S., and Miller, W. A. (2008) *RNA* **14,** 134–147
36. Miller, W. A., and Giedroc, D. P. (2009) in *Recoding: Expanded decoding rules enrich gene expression* (Atkins, J. F., and Gesteland, R. F., eds) Springer-Verlag, in press
37. Taliansky, M. E., and Robinson, D. J. (2003) *J. Gen. Virol.* **84,** 1951–1960
38. Demler, S. A., Rucker, D. G., and de Zoeten, G. A. (1993) *J. Gen. Virol.* **74,** 1–14
39. Demler, S. A., Rucker-Feeney, D. G., Skaf, J. S., and de Zoeten, G. A. (1997) *J. Gen. Virol.* **78,** 511–523
40. Rakotondrafara, A. M., Jackson, J., Pettit Kneller, E. J., and Miller, W. A. (2007) in *Current Protocols in Microbiology* (Coico, R., Towalik, T., Quaries, J., Stevenson, B., and Taylor, R., eds) pp. 16D.3.1–16D.3.12, John Wiley & Sons, New York
41. Merino, E. J., Wilkinson, K. A., Coughlan, J. L., and Weeks, K. M. (2005) *J. Am. Chem. Soc.* **127,** 4223–4231
42. Wilkinson, K. A., Merino, E. J., and Weeks, K. M. (2006) *Nat. Protoc.* **1,** 1610–1616
43. Zuker, M. (2003) *Nucleic Acids Res.* **31,** 3406–3415
44. Mayberry, L. K., Dennis, M. D., Leah Allen, M., Ruud Nitka, K., Murphy, P. A., Campbell, L., and Browning, K. S. (2007) *Methods Enzymol.* **430,** 397–408
45. Monzingo, A. F., Dhaliwal, S., Dutt-Chaudhuri, A., Lyon, A., Sadow, J. H., Hoffman, D. W., Robertus, J. D., and Browning, K. S. (2007) *Plant Physiol.* **143,** 1504–1518
46. Bradford, M. M. (1976) *Anal. Biochem.* **72,** 248–254
47. Morino, S., Hazama, H., Ozaki, M., Teraoka, Y., Shibata, S., Doi, M., Ueda, H., Ishida, T., and Uesugi, S. (1996) *Eur. J. Biochem.* **239,** 597–601
48. Wong, I., and Lohman, T. M. (1993) *Proc. Natl. Acad. Sci. U. S. A.* **90,** 5428–5432
49. Barry, J. K., and Miller, W. A. (2002) *Proc. Natl. Acad. Sci. U. S. A.* **99,** 11133–11138
50. Wang, S., Browning, K. S., and Miller, W. A. (1997) *EMBO J.* **16,** 4107–4116
51. Jeffrey, S. B., Benedicte, D., Yoshimi, Y., and Karen-Beth, G. S. (2006) *FEBS Lett.* **580,** 2591–2597
52. Guo, L., Allen, E. M., and Miller, W. A. (2001) *Mol. Cell* **7,** 1103–1109
53. Gallie, D. R. (2002) *Nucleic Acids Res.* **30,** 3401–3411
54. Zeenko, V., and Gallie, D. R. (2005) *J. Biol. Chem.* **280,** 26813–26824
55. Allen, M. L., Metz, A. M., Timmer, R. T., Rhoads, R. E., and Browning, K. S. (1992) *J. Biol. Chem.* **267,** 23232–23236
56. Browning, K. S. (2004) *Biochem. Soc. Trans.* **32,** 589–591
57. Richter, J. D., and Sonenberg, N. (2005) *Nature* **433,** 477–480
58. Dever, T. E. (2002) *Cell* **108,** 545–556
59. Pestova, T. V., Kolupaeva, V. G., Lomakin, I. B., Pilipenko, E. V., Shatsky, I. N., Agol, V. I., and Hellen, C. U. T. (2001) *Proc. Natl. Acad. Sci. U. S. A.* **98,** 7029–7036
60. Sonenberg, N., and Dever, T. E. (2003) *Curr. Opin. Struct. Biol.* **13,** 56–63
61. Tomoo, K., Shen, X., Okabe, K., Nozoe, Y., Fukuhara, S., Morino, S., Ishida, T., Taniguchi, T., Hasegawa, H., Terashima, A., Sasaki, M., Katsuya, Y., Kitamura, K., Miyoshi, H., Ishikawa, M., and Miura, K.-i. (2002) *Biochem. J.* **362,** 539–544
62. Tomoo, K., Shen, X., Okabe, K., Nozoe, Y., Fukuhara, S., Morino, S., Sasaki, M., Taniguchi, T., Miyagawa, H., Kitamura, K., Miura, K.-i., and Ishida, T. (2003) *J. Mol. Biol.* **328,** 365–383
63. Niedzwiecka, A., Marcotrigiano, J., Stepinski, J., Jankowska-Anyszka, M., Wyslouch-Cieszynska, A., Dadlez, M., Gingras, A.-C., Mak, P., Darzynkiewicz, E., Sonenberg, N., Burley, S. K., and Stolarski, R. (2002) *J. Mol. Biol.* **319,** 615–635

64. Rutkowska-Wlodarczyk, I., Stepinski, J., Dadlez, M., Darzynkiewicz, E., Stolarski, R., and Niedzwiecka, A. (2008) *Biochemistry* **47,** 2710–2720
65. Mochizuki, K., Oguro, A., Ohtsu, T., Sonenberg, N., and Nakamura, Y. (2005) *RNA* **11,** 77–89
66. Nieto, C., Morales, M., Orjeda, G., Clepet, C., Monfort, A., Sturbois, B., Puigdomenech, P., Pitrat, M., Caboche, M., Dogimont, C., Garcia-Mas, J., Aranda, M. A., and Bendahmane, A. (2006) *Plant J.* **48,** 452–462
67. Truniger, V., Nieto, C., Gonzalez-Ibeas, D., and Aranda, M. (2008) *Plant J.* **56,** 716–727
68. Schaad, M. C., Anderberg, R. J., and Carrington, J. C. (2000) *Virology* **273,** 300–306
69. German-Retana, S., Walter, J., Doublet, B., Roudet-Tavert, G., Nicaise, V., Lecampion, C., Houvenaghel, M.-C., Robaglia, C., Michon, T., and Le Gall, O. (2008) *J. Virol.* **82,** 7601–7612
70. Robaglia, C., and Caranta, C. (2006) *Trends Plant Sci.* **11,** 40–45
71. Niepel, M., Ling, J., and Gallie, D. R. (1999) *FEBS Lett.* **462,** 79–84
72. Miller, W. A., and White, K. A. (2006) *Annu. Rev. Phytopathol.* **44,** 447–467
73. Meulewaeter, F., Van Montagu, M., and Cornelissen, M. (1998) *RNA* **4,** 1347–1356
74. Qu, F., and Morris, T. J. (2000) *J. Virol.* **74,** 1085–1093
75. Stupina, V. A., Meskauskas, A., McCormack, J. C., Yingling, Y. G., Shapiro, B. A., Dinman, J. D., and Simon, A. E. (2008) *RNA* **14,** 2379–2393
76. Scheets, K., and Redinbaugh, M. G. (2006) *Virology* **350,** 171–183